Physiological
Measurement

PAPER • **OPEN ACCESS**

LumEDA: image luminance based contactless correlates of electrodermal responses

To cite this article: Mayur Bhamborae *et al* 2025 *Physiol. Meas.* **46** 025010

IOP Publishing Physiol. Meas. 46 (2025) 025010 https://doi.org/10.1088/1361-6579/adb369

Physiological Measurement

IPEM Institute of Physics and Engineering in Medicine

OPEN ACCESS

RECEIVED
17 June 2024

REVISED
2 January 2025

ACCEPTED FOR PUBLICATION
6 February 2025

PUBLISHED
20 February 2025

PAPER

LumEDA: image luminance based contactless correlates of electrodermal responses

Mayur Bhamborae[1,*], Elena N Schneider[1], Philipp Flotho[1], Alexander L Francis[2] and Daniel J Strauss[1]

[1] Systems Neuroscience and Neurotechnology Unit, Faculty of Medicine, Saarland University and School of Engineering, htw saar, Homburg/Saar, Germany

[2] Speech Perception and Cognitive Effort (SPACE) Lab, Dept. of Speech, Language & Hearing Sciences, Purdue University, West Lafayette, IN, United States of America

[*] Author to whom any correspondence should be addressed.

E-mail: mayur.bhamborae@uni-saarland.de

Keywords: contactless, electrodermal activity (EDA), galvanic skin response (GSR), skin conductance (SC)

Supplementary material for this article is available online

Abstract

Objective. Electrodermal activity (EDA) is a marker of psychophysiological arousal and is usually a measure of the skin conductance which is associated with sweat gland activity. Recent studies have shown that it is possible to estimate the EDA using contactless video based methods. *Approach*. Sensor EDA signals (SenEDA) and videos of the the palm were recorded simultaneously from over 30 participants under various stimuli (audio, video, cognitive and physiological). The luminance information from the video data was used to track sweat gland activity on the skin surface and extract the contactless signal luminance based EDA (LumEDA). *Main results*. Comparison of the SenEDA and LumEDA signals showed a high positive correlation between the two as expected. *Significance*. Under suitable illumination, simple spatial filters can be used to track sweat gland activity which can then be used to estimate signals analogous to the EDA. Such video based methods also facilitate spatio-temporal analysis of EDA correlates over larger areas of the body.

1. Introduction

Electrodermal activity (EDA) is a measure of the changes in the electrical properties of the skin due to eccrine sweat gland activity regulated by the sympathetic nervous system (SNS). EDA is widely used as a marker of emotional arousal and is therefore used in psychophysiological studies. Traditional measurement of EDA requires sensors (usually consisting of two electrodes) that are in electrical contact with skin surface, and this is commonly done at sites that have a higher concentration of eccrine sweat glands such as the palm (Boucsein 2012).

EDA continues to be the most widely used biosignal in psychophysiological studies (Posada-Quintero and Chon 2020). The emergence of low-cost consumer wearable devices with skin conductance measuring capabilities has democratized the monitoring of EDA beyond laboratory or clinical applications. However, in some situations, placing these contact-based sensors may not be possible, therefore a contactless approach that estimates correlates of EDA would be the next best alternative. Sensor-based EDA measurements also cover only a small area of the skin and therefore have a relatively low spatial resolution. A contactless approach has the potential to offer much higher spatial resolution for EDA measurement as it can cover a larger area of the skin at the same time and can therefore help in further understanding the electrodermal system and the functioning of the SNS.

Camera-based contactless monitoring of physiological vital signs has become ubiquitous with the widespread availability of low-cost camera systems and is ever increasing in popularity since the COVID-19 pandemic with the need for contactless alternatives to monitoring patients from a distance (Flotho *et al* 2021). Conceptually, these methods track changes in the appearance of the skin which occur due to variations in the dermal blood volume corresponding to cardiovascular function (Wu *et al* 2000). These

changes may be invisible to the naked eye, but with digital camera systems, they can be quantified using pixel intensity variations over time. These contactless methods are based on multi-channel (colour) information or single channel (greyscale) based depending on the underlying method used. A state-of-the-art overview of camera based physiological monitoring can be found in (McDuff 2023).

EDA and the number of active sweat glands in a given area, known as the palmar sweat index (PSI), are positively correlated (Sutarman and Thompson 1952, Turpin and Clements 1993, Freedman *et al* 1994). PSI based methods require visual analysis of the surface of the skin, and older studies such as Köhler and Schuschel (1994) use pigments, tapes, or other chemical substances to create impressions of sweating skin, resulting in poor temporal resolution of the analyses. Recent advances in machine vision and computational photography facilitate similar analyses at much higher temporal resolution without the use of any pigments or chemicals. Contactless methods have been previously reported albeit using laboratory equipment such as video-microscopy (Nishiyama *et al* 2001), optical coherence tomography (Nohara *et al* 2005) and thermal imaging using high-end thermal cameras (Krzywicki *et al* 2014). However, all of these methods require expensive equipment. The use of contactless, high spatial resolution EDA measures would be greatly advanced by the availability of a technique that uses commonly available and inexpensive RGB cameras to analyse EDA on the surface of the skin.

Bhamborae *et al* (2020) showed for the first time that under suitable illumination conditions, contactless, video-based correlates of electrodermal responses can be estimated using simple image filters because sweat droplets which appear on skin reflect light differently compared to the surrounding skin surface and therefore appear as bright dots in the image. Following this, the findings of Braun *et al* (2023) showed that sympathetic arousal can be measured using the remote photoplethysmography signal extracted from RGB videos. However, these studies rely on using strong physiological stimuli such as deep breathing exercise in Krzywicki *et al* (2014), Valsalva Manoeuvre in Bhamborae *et al* (2020) and self-pinching in Braun *et al* (2023). With the primary goal of being able to determine if similar effects could be observed across a variety of stimuli and a larger, more diverse population, the study reported here uses an improved method with more natural position of the hand and a paradigm that employs auditory, visual, cognitive and physiological stimuli to evoke electrodermal responses.

2. Materials and methods

2.1. Participants

The study included 41 healthy adult participants (21 females; mean age = 29.44 years, SD = 6.42 years, range: 22–51 years). They were all asked to refrain from alcoholic or caffeinated beverages 24 h before the measurement. The study was performed in accordance with the Declaration of Helsinki and was approved by the Saarland State Medical Association, Ärztekammer des Saarlandes (Approval:47/18). All participants provided written informed consent to participate in this study.

2.2. Protocol

Following a 5 minute acclimation period to establish baseline measurements, the experimental protocol consisted of four distinct components-visual, auditory, cognitive, and physiological stimulation-with adequate rest periods between each phase to facilitate recovery.

Visual stimulation: ten grey value intensity normalized images from the International Affective Picture System (IAPS) (Lang *et al* 2005) were shown for 7 s each on a computer screen as visual stimuli. To avoid habituation, the inter-stimulus interval (ISI) alternated randomly between 40 and 60 s. The screen showed a neutral, all-grey frame during these intervals.

Auditory stimulation: ten brief audio snippets from the International Affective Digitized Sounds (2nd Edition; IADS-2) (Bradley and Lang 2007) were played for 7 s as part of the auditory stimulation. The ISI varied randomly between 40 and 60 s. During the entire part, participants were asked to look at a fixation cross on the screen. The audio system was calibrated to a sound pressure level 60 dB.

Cognitive Stimulation: consisted of two distinct parts-an imaginative exercise followed by an arithmetic task. For the imaginative part, participants were asked to imagine a unpleasant (negative) situation, and then a situation which made them happy (positive). Following this was a 300 s long descending subtraction task where the participants had to count down in steps of 7 starting from 1001. Adequate breaks were provided between each section for recovery.

Physiological stimulation: participants had to perform the Valsalva Manoeuvre five times for 10 s with a 15 s preparation time before each trial. A recovery period of 60 s was provided between each trial.

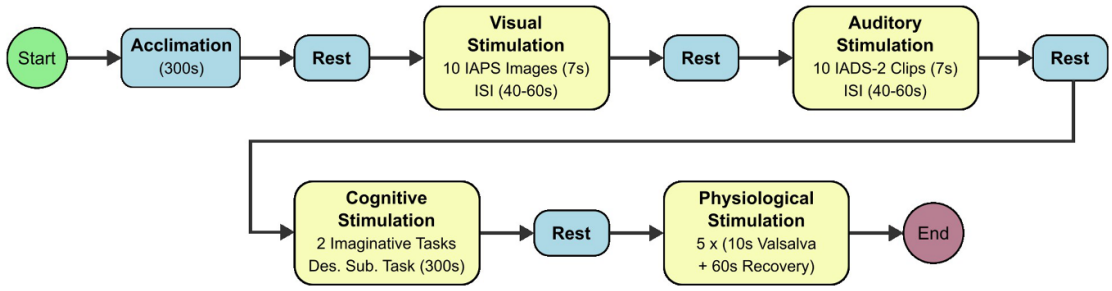

Figure 1. Overview of the experimental protocol. A variety of different stimuli were used to elicit electrodermal responses from participants. Participants were free to rest as long as necessary between the different stages of the experiment. An entire session lasted for about 60 min on average.

Measurements were conducted in a climate controlled room. Participants were seated on an ergonomic cushioned office chair facing a 27 inch colour monitor placed 180 cm away. All instructions and countdowns were displayed on the screen throughout the measurement, and participants had to provide verbal confirmation to proceed after the breaks between each of the above mentioned phases of the experiment. Figure 1 illustrates the entire timeline of the experimental protocol.

2.3. Data acquisition

Sources of the experimental data in this study consist of a contactless source and a contact-based source. The contact-based data sensor EDA (SenEDA) serves as the ground truth (reference/control) against which the data acquired from the video data luminance based EDA (LumEDA) are compared.

SenEDA

The ground truth SenEDA was recorded as a measurement of exosomatic skin conductance (with 400 mV DC) using a sensor (g.GSR) and biosignal amplifier (g.USBAMP). A sampling rate of 356 Hz was used. The sensors were placed in contact with the palmar side of the middle phalanges of the ring and the middle fingers of the left hand. A multimodal trigger box (g.TRIGBOX) was used to enable synchronization between the various equipment involved in the experiment. The sensor, biosignal amplifier, and trigger box were manufactured by g.tec medical engineering GmbH, Austria.

Video data

The vision system consisted of a 12.4 Megapixel (4112 × 3008) machine vision camera (Ximea GmbH MC124CG-SY) fitted with a 16 mm F1.8 lens (Kowa LM16FC24M) pointing upwards.The participants placed their left palm pronated on a support frame mounted on a metal construction with cushioned forearm support. Illumination was provided by three different light sources (Cameo Q-SPOT 15 RGBW) arranged in an arc 50 cm from the palm rest. The lights were activated one at a time using DMX-512 signals, synchronized with video frames, creating a time division multiplexed illumination sequence. This construction was covered in blackout fabric to block off external light and to prevent it from interfering with the participants. Camera data was recorded with full spatial resolution and saved in raw, colour filter array 8-bit data depth format along with timestamps and the light associated with each frame. Figure 2 shows the setup used with the blackout cover removed. Light 1 was on the thenar (thumb) side of the palm, Light 2 pointed straight up and Light 3 was on the hypothenar side of the palm. Light 1 and Light 3 illuminate the palm at an angle. Figure 3 contains samples frames of the palm illuminated by the three different lights.

Extracting LumEDA

Grazing incidence imaging in combination with computational photography is widely used in artistic and scientific applications (Kajiya *et al* 2014, Xiao *et al* 2019) as it offers better contrast and surface texture sensitivity. Eccrine sweat glands, activated during psychological or physiological arousal, secrete sweat onto the skin surface, creating textural changes that appear as bright dots due to specular reflection. These droplets contrast sharply with the otherwise light-absorbing dry skin (see figure 4), making it feasible to isolate them for further processing. Since surface sweat correlates positively with EDA, analysing these bright spots provides a method for measuring EDA levels.

The frames from the three light sources were combined using a maximum intensity approach, wherein each pixel in the resulting image was assigned the highest value found among the three sources (see figure 3(d)). A manually selected region of interest (ROI) was then tracked automatically using the Kernelized cross-correlation tracker (Henriques *et al* 2014).

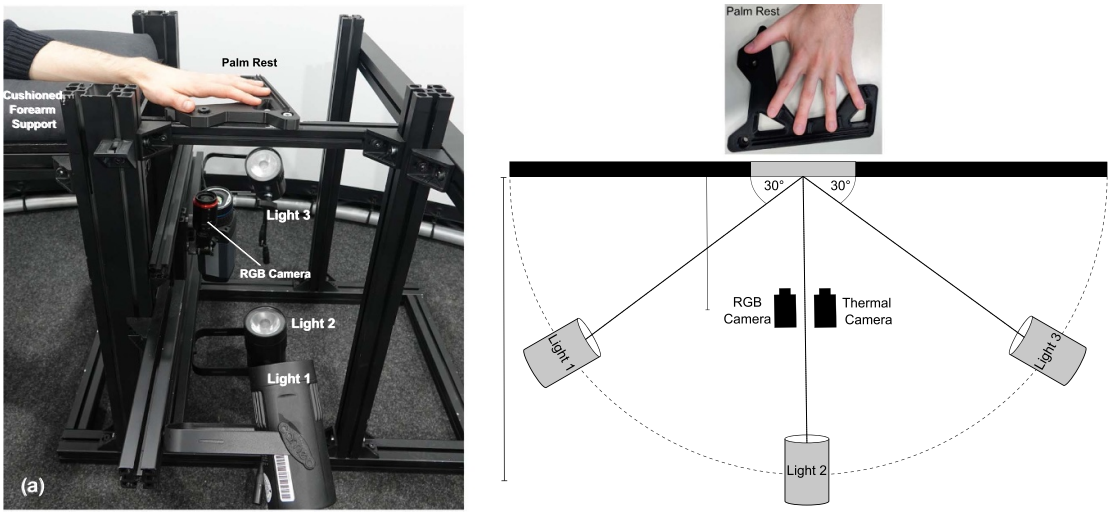

Figure 2. (a) Image of the setup with the camera, light and palm-rest arrangement with the blackout fabric removed. (b) Schematic of the vision system and its position with respect to the palm.

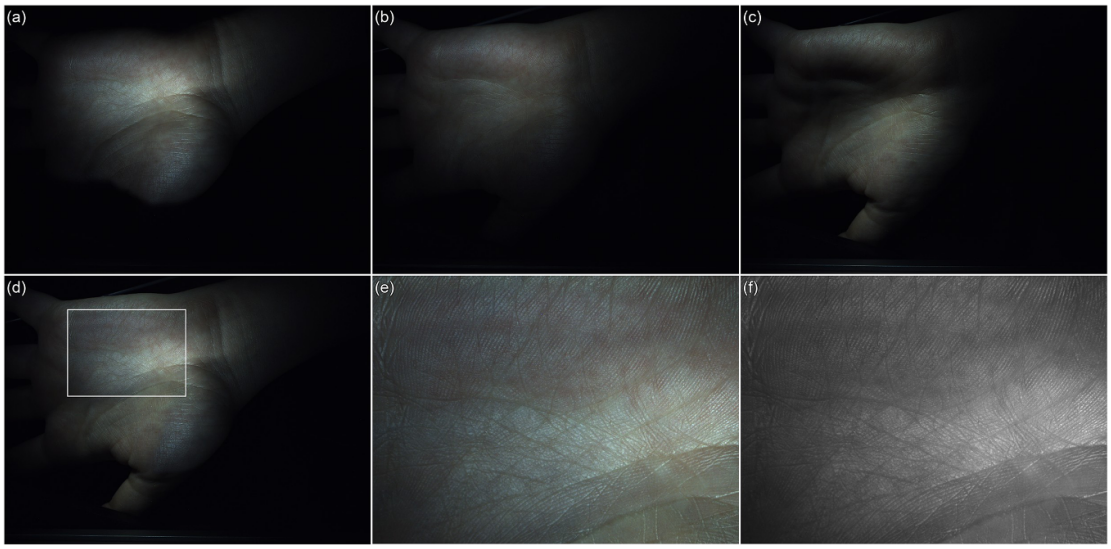

Figure 3. *Top*: three consecutive frames from the recording. Each frame is associated with only one light source, (a), (b) and (c) are associated with Light 1, Light 2 and Light 3 respectively. *Bottom*: (d) maximum intensity fusion and ROI Selection. (e) Selected ROI. (f) Luminance image of selected ROI.

The YCbCr color space is a non-linear colour space and represents the greyscale brightness (luminance, Y) and the colour (chrominance: Cb and Cr) information. Since only the changes in brightness of the pixels are of interest, the Y-channel of the YCbCr space was used to extract the luminance information from the RGB frames. Sweat dots are then detected using the Laplacian filter, which is a spatial high-pass filter that emphasizes rapid intensity changes while suppressing slowly varying features. A binary image containing just the sweat dots was then obtained by using a thresholding operation. This binary image was then morphologically dilated using a disk shaped structuring element to enhance the sweat dots (see figure 4(f)). Finally, the total number of non-zero pixels in this binary image, normalized by the size of the ROI was used as the sample intensity for the LumEDA signal. Figure 5 gives an overview of these steps. Sample video clips from the study are available in the supplementary materials.

2.4. Data synchronization and epoch extraction

To compare the responses captured using the camera-based method (LumEDA) with the ground truth sensor data (SenEDA), the sensor data was first converted to microsiemens and then resampled to 4 Hz (to match the sampling frequency of the LumEDA signal). The signals were then Butterworth low-pass filtered

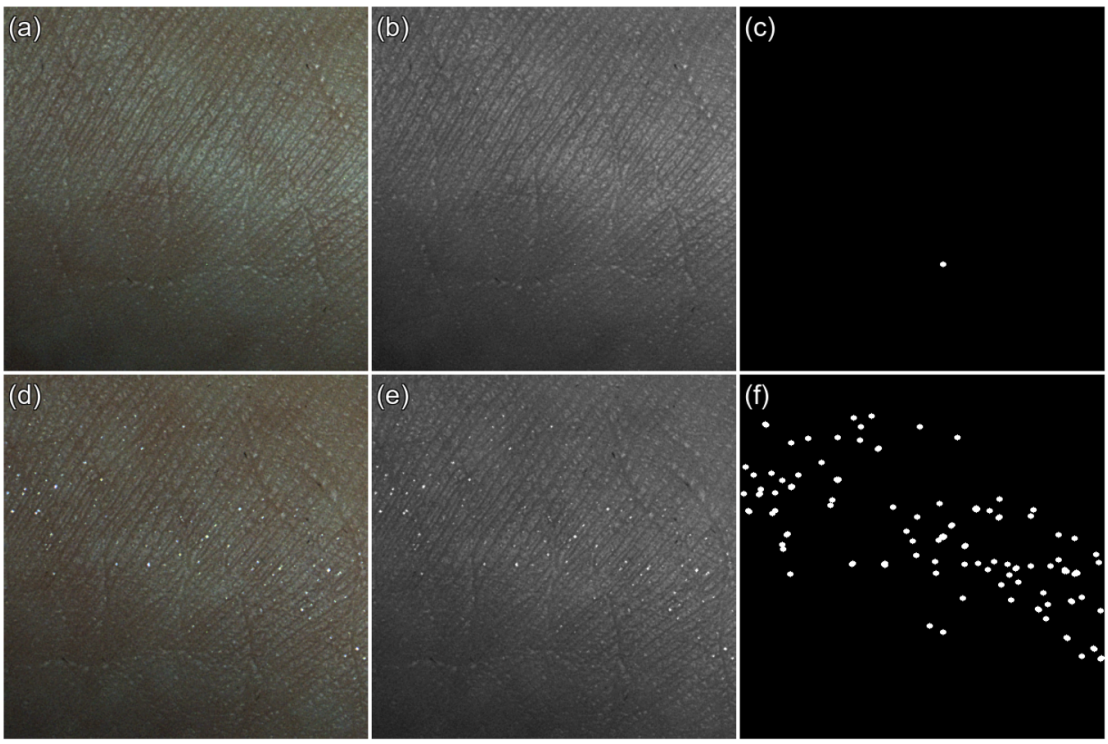

Figure 4. *Top* (a) Sample frame (b) luminance (c) mask during low arousal. *Bottom* (d) Frame during high arousal. Surface sweat can be seen as bright dots. (e) Luminance from which LumEDA is extracted. (f) Mask after enhancing the bright dots using morphological dilation.

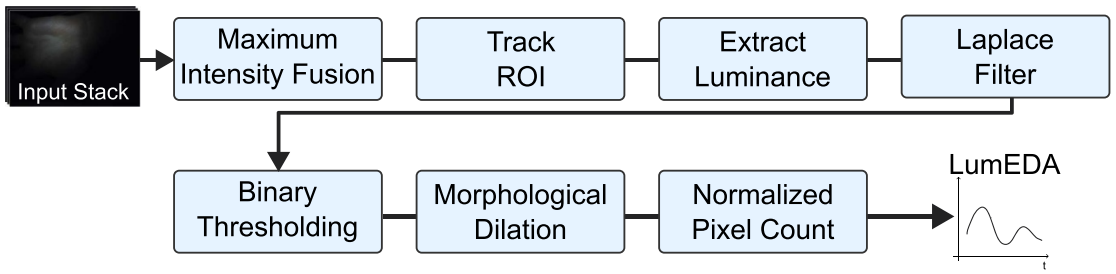

Figure 5. Overview of the steps to compute the image luminance based EDA (LumEDA) signal.

(2nd order, cut-off 0.5 Hz). Alignment was then done using synchronization triggers exchanged between the data acquisition programs.

For event based analysis around specific stimuli (visual and auditory), epochs of 30 s (10 s before the event and 20 s after) were extracted. The mean of the 10 s before the event was taken as the baseline and then subtracted, therefore no further decomposition (into phasic or tonic components) or detrending of the signals was necessary. For analysing longer intervals (cognitive and physiological stimuli), the signals were low-pass filtered with a cut-off frequency of 0.1 Hz to retain the tonic components.

2.5. Automated electrodermal response (EDR) detection

For the epochs created from the responses to the visual and auditory stimuli, automated peak detection using the z-score (signals are rescaled to have a mean of 0 and a standard deviation of 1) of the mean response of SenEDA and LumEDA of each participant was performed to enable a comparison of EDR parameters such as latency and intensity (amplitude) variations. For a peak to be considered an EDR, a minimum peak amplitude of 0.01 had to be reached (Boucsein 2012). Since electrodermal responses to events are slow, only peak latencies in an interval between 1 s up to 5 s are considered (Boucsein 2012). In the present case, latencies from the stimulus onset up to 8 s after the stimulus are considered to account for any misalignment between the signals. Due to the relatively strong fluctuations in the LumEDA, a Fourier function was fitted to

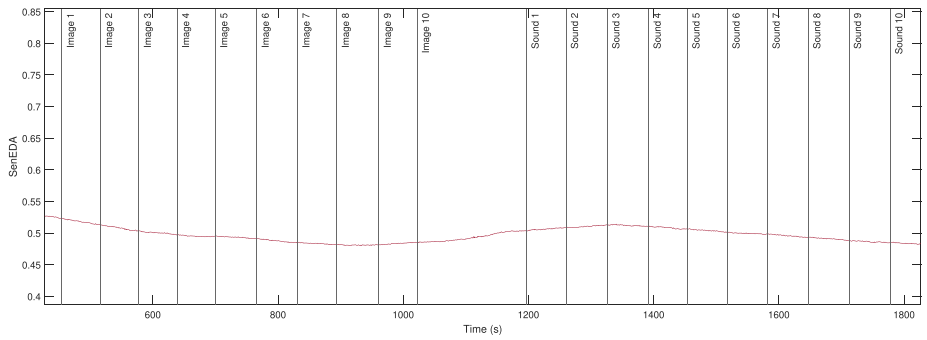

Figure 6. An example of a non-responder. It can be seen here that this participant did not show the expected response to stimuli in the ground truth (SenEDA) signal. Such participants were excluded from comparisons.

the data using MATLAB curve fitter. The Pearson correlation coefficient between latency and amplitude values in both SenEDA and LumEDA signals were then computed.

3. Data analysis and results

Data collection from 2 participants was terminated due to technical issues, leaving with data from 39 (21 females) participants to be analysed. The data from each stage (visual, auditory, cognitive and physiological) of the experiment were then analysed separately. *non-responders* were identified as those who did not show an expected response in the SenEDA signal and such participants excluded from comparisons as the goal of this study was to compare the LumEDA signals against the ground truth SenEDA signal. An example non-responder can be seen in figure 6. A total of 10 non-responders were identified for the visual and auditory sections resulting in a sample size of 31 participants (16 females, 15 males) for event based analysis. For the cognitive and physiological stimulation, 38 participants (19 female, 19 male) were analysed as one session had to be aborted after the auditory stimulation due to technical failure.

For the event based analysis, only the single responses, i.e. the 30 s epochs around the events were used. To compare the two signals, a samplewise t-test was performed using the normalized grand average responses and corrected using false discovery rate of 0.05 (Benjamini and Hochberg 1995, Benjamini and Yekutieli 2001, 2005). Figures 7 and 8 show the responses to visual stimuli and auditory stimuli respectively.

Figure 9 shows a comparison of a participant's LumEDA and SenEDA responses to cognitive and physiological stimuli. For the cognitive and physiological stimuli, the entire signal was used since there were no specific events. The average correlation across participants was calculated using the Fisher transformation method.

3.1. Visual stimuli

On average, the participants showed a weak response to visual stimuli as seen in figure 9(a). Female participants were only slightly more responsive to the visual stimuli than male participants. Plots for comparison can be found in the supplementary material. A moderate positive Pearson correlation of $r = 0.53$ with $p < 0.01$ was seen between the averaged LumEDA and SenEDA responses to visual stimuli. A comparison of the correlation coefficient for male and female participants can be found in table 1.

3.2. Auditory stimuli

Figure 8 shows the responses of a participant to auditory stimuli. Participants exhibited stronger responses to auditory stimuli compared to visual stimuli (compare figures 10(a) and (b)). These stronger responses also meant higher intensities in the LumEDA signal. The LumEDA signal was also positively correlated with the SenEDA signal ($r = 0.92$ $p < 0.01$). Female and male participants responded similarly to auditory stimuli.

3.3. Cognitive stimuli

Both female and male participants showed similar responses to cognitive stimulation. On average, a high positive ($r = 0.64$ $p < 0.01$) correlation was seen between the SenEDA and LumEDA signals. Table 2 gives an overview of this. Figure 11 provides an overview of the responses of all 38 participants.

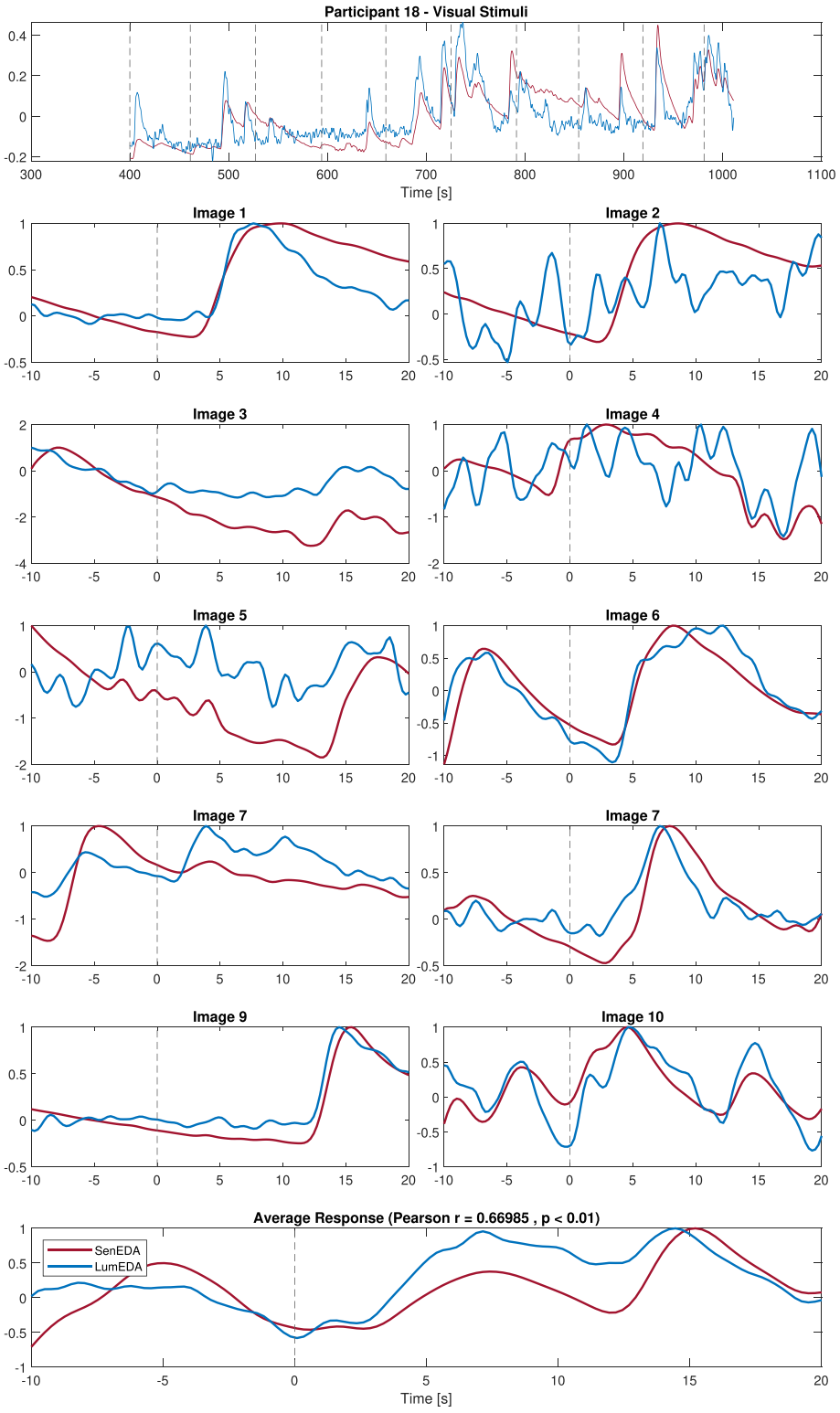

Figure 7. Responses to visual stimuli (Participant 18).

3.4. Physiological stimuli

On average, a high positive ($r = 0.70$ $p < 0.01$) correlation was seen between the SenEDA and LumEDA signals. Table 2 shows that there was not a significant difference between male and female participants. Responses of all participants can be seen in figure 12.

3.5. Latency and amplitude comparisons

Figure 13 presents a scatter plot analysing the relationship between amplitude and latency in event-related electrodermal responses (visual and auditory stimuli) from the SenEDA and LumEDA signals. Analysis of

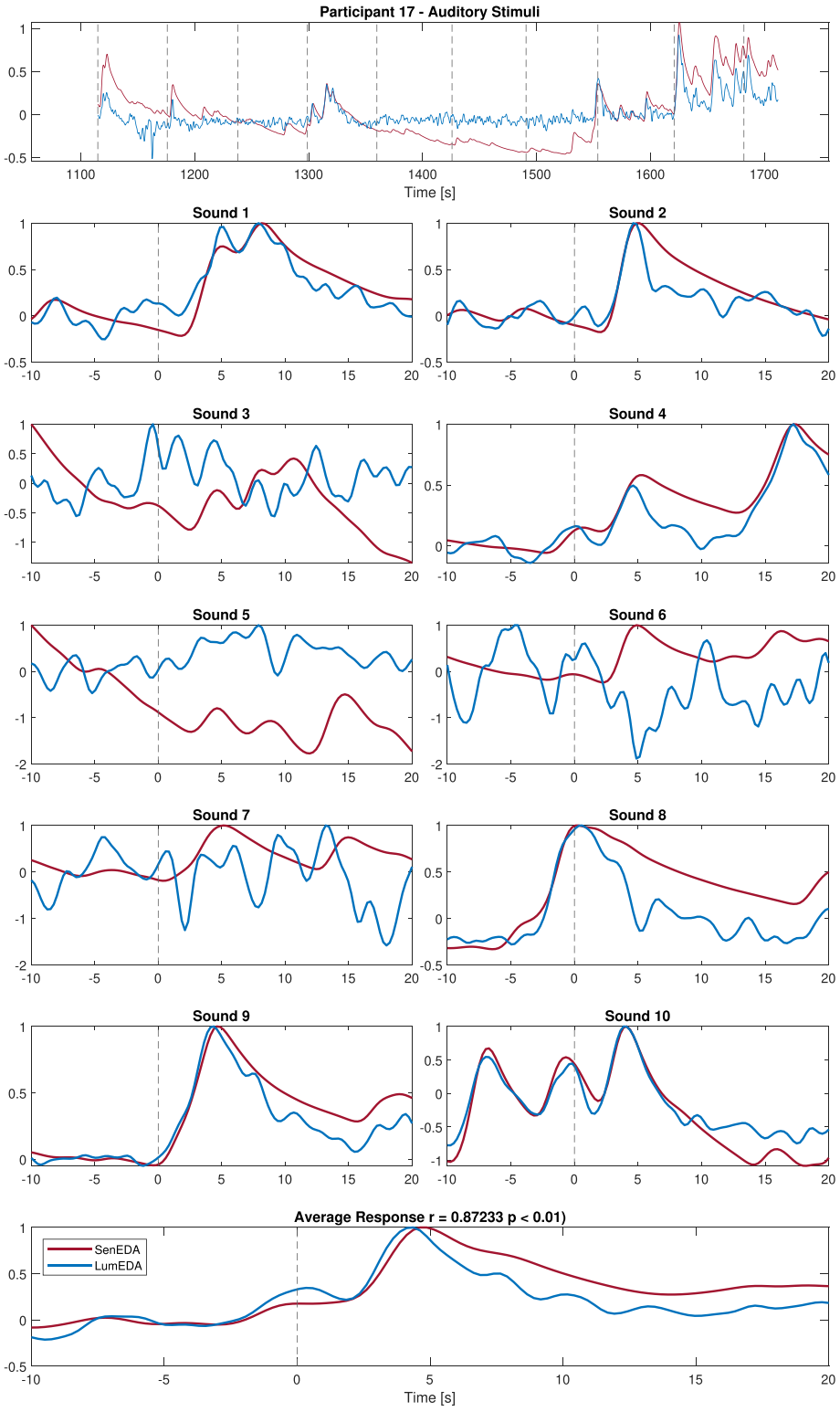

Figure 8. Responses to auditory stimuli (Participant 17).

620 responses (20 responses each from 31 participants) revealed a moderate positive correlation ($r = 0.55$) for amplitude values, while latency measurements showed no significant correlation between the two methods. EDR amplitudes are commonly analysed to evaluate arousal responses to stimuli and this case, LumEDA signals do show good consistency with the SenEDA signals. The same cannot be said in the case of EDR latencies for a variety of reasons. An important one being the nature of the camera based LumEDA signal which is extracted from only visible changes on the skin surface whereas the sensor based signal which can measure changes even under the surface. Another reason could be the difference in the location where the

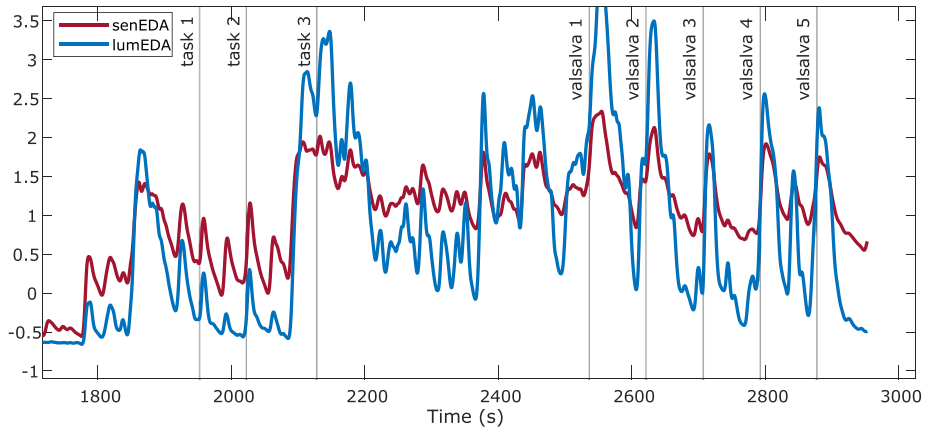

Figure 9. SenEDA vs. LumEDA for cognitive and physiological stimulation for an exemplary participant.

Table 1. Average Pearson correlation coefficients for visual and auditory stimuli calculated by averaging the single responses.

	Female	Male	All
Sample size	*15*	*16*	*31*
Visual	0.36	0.29	0.53
Auditory	0.96	0.85	0.92
All	0.91	0.85	0.94

LumEDA and SenEDA signal originate from. LumEDA was extracted from the palm, whereas the SenEDA from the fingers. Despite using manual assist the automatic peak detection, accurate peak identification remains challenging due to small signal fluctuations in LumEDA and potential alignment inconsistencies between the two signals. Furthermore, the extended time window used to accommodate these challenges may have inadvertently included peaks outside the typical response window for stimulus-related activity.

4. Discussion

4.1. The Average LumEDA and SenEDA responses are positively correlated

A strong positive correlation is to be expected since the LumEDA signal, analogous to the PSI, is based on being able to capture sweat gland activity on the skin surface, which is known to be correlated with the EDA. However, it is also important to mention that the algorithm used to extract the LumEDA depends on changes to the texture of the skin surface due to the appearance and disappearance of sweat droplets caused by evaporation and reabsorption of these sweat droplets (Baker 2019). This method does not respect skin colour changes due to peripheral blood flow variations as in Braun *et al* (2023) and therefore has very little contribution from changes that occur beneath the surface of the skin.

4.2. Large inter-subject variability

A closer look at the signals reveals a large inter-subject variability between participants, which is common to studies involving EDA (Posada-Quintero *et al* 2016a). This is reflected in the LumEDA signals even more strongly due to distortions caused by motion and participants inadvertently moving their hands, affecting the validity of initial camera settings (e.g. camera focus and the illumination angles) in later computations. Another reason for this is that LumEDA primarily tracks changes that occur on the skin surface but not all participants may have had responses strong enough for sweat droplets to appear on the skin. In such cases, a contact-based sensor would likely still have been able to measure changes in skin conductance. Due to the nature of the optical setup used in this study, the variance in the palm size of participants also meant that the palm rest was not optimal in all cases as their palms were not optimally placed for the duration of the measurement, leading to inconsistencies of LumEDA signal extracted.

Another important aspect to consider is the difference in skin texture, hydration levels and the humidity in the measurement room over the duration of the entire study. These factors are known to have an impact on electrodermal recordings (Boucsein 2012). Since the camera based LumEDA signal depends on the appearance and quick reabsorption and evaporation of the tiny sweat droplet on the surface of the of skin, the hydration levels of the participant's palmar skin, the ambient humidity and temperature during the

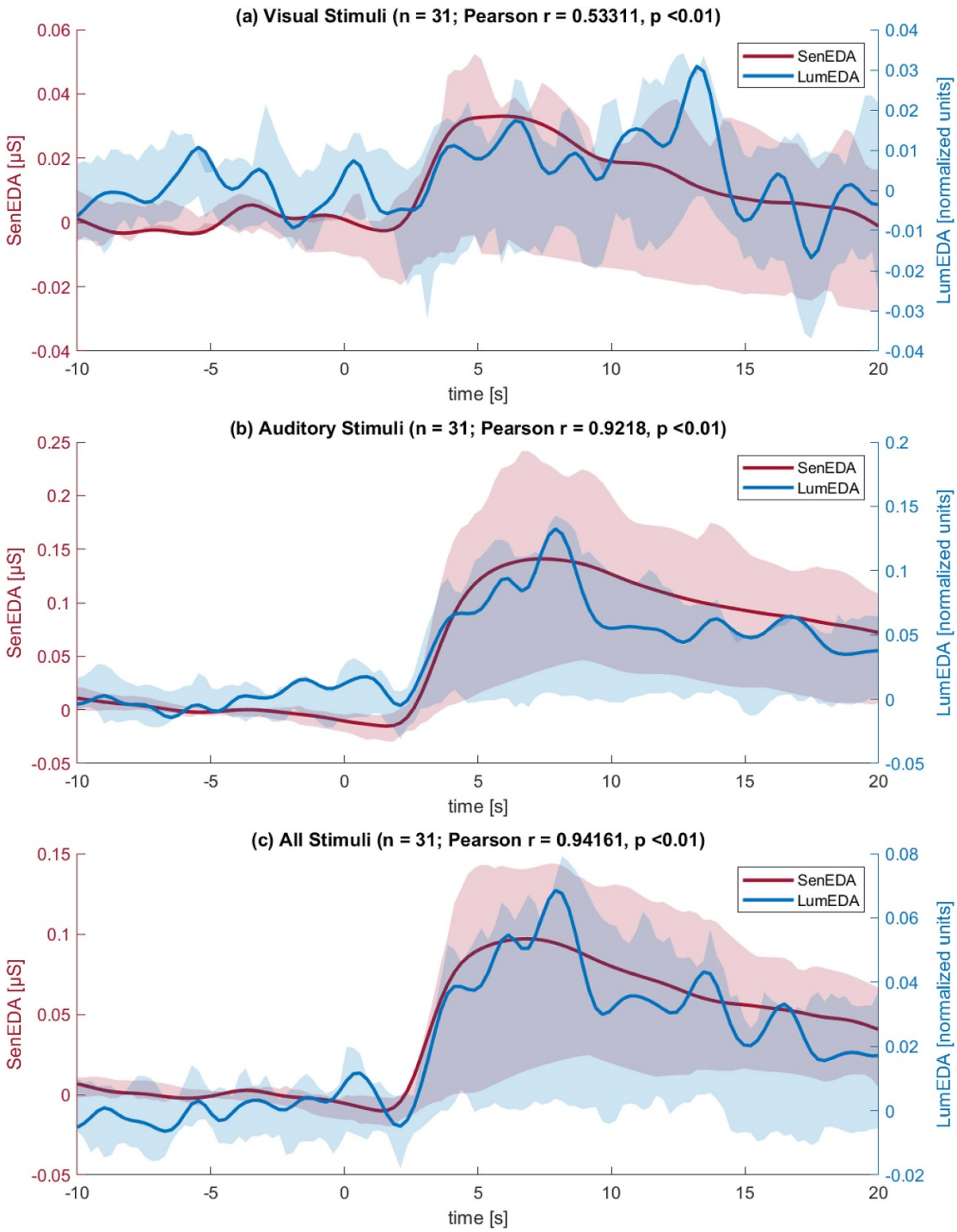

Figure 10. Comparison of the mean responses to (a) visual stimuli, (b) auditory stimuli and the (c) grand average across visual and auditory stimuli. (Sample size = 31).

Table 2. Average Pearson correlation coefficients for cognitive and physiological stimuli calculated by using the Fisher transformation method.

	Female	Male	All
Sample size	*19*	*19*	*38*
Cognitive	0.69	0.62	0.64
Physiological	0.71	0.70	0.70

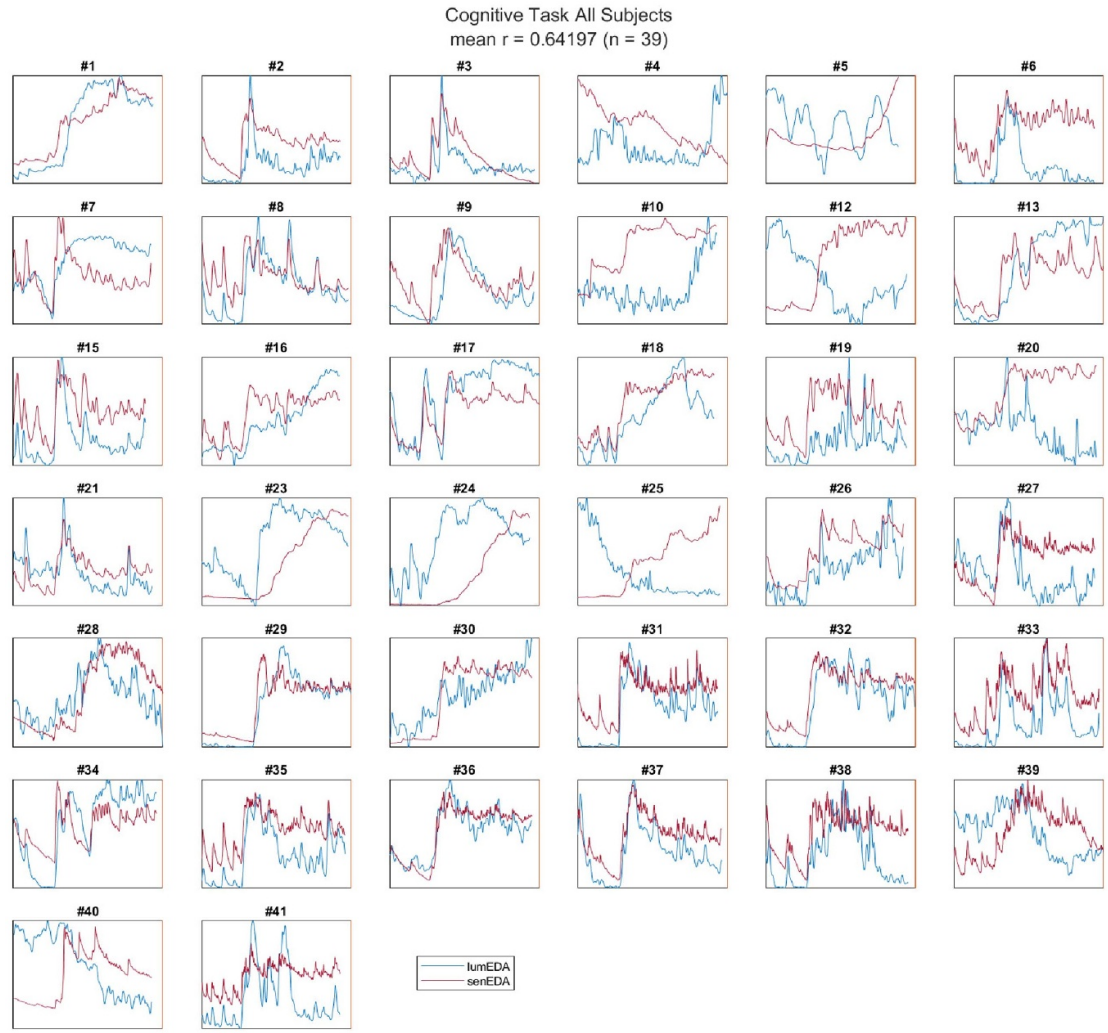

Figure 11. Overview of the SenEDA and LumEDA responses to cognitive stimuli (imagination task + descending subtraction task).

measurement, and the duration of the ISI can all affect the LumEDA. Figure 14 exemplifies the variation in skin texture and hydration as seen in the video data. The Laplacian, which is the sum of the second order spatial derivates of an image is highly sensitive to noise and changes in surface texture. Since the LumEDA involved the computation of the Laplacian and it was done with the same parameters for all participants, this could result in suboptimal identification of the sweat dots in some cases. While false detection due to static features such as fingerprints can be mitigated by removing the mean, additional motion can introduce artefacts that can be hard to filter out.

4.3. Absence of tonic information in LumEDA

The EDA signals consist of two components, the fast-changing phasic component and a slow-changing tonic component. The method used to extract the LumEDA depends explicitly on the appearance of tiny sweat particles on the surface of the skin, which disappear again in a very short time scale, and is therefore not as reliable for capturing tonic activity over time. However, methods that consider chromatic information and also use a more realistic model of the skin, such as (Baranoski and Krishnaswamy 2010), may be able to capture tonic electrodermal information using video data as they consider not just surface level characteristics but also sub-surface interaction of light with skin. On the other hand, the phasic component is most used for detecting event related arousal and it has been previously shown that this high frequency phasic component provides better inter-subject comparability and that sympathetic arousal is better captured in the phasic component (Posada-Quintero *et al* 2016a, 2016b).

4.4. LumEDA and motion

The complete measurement paradigm also included other tasks involving emotional, cognitive and physiological stimuli. However, since several participants took out their hands during the break between the

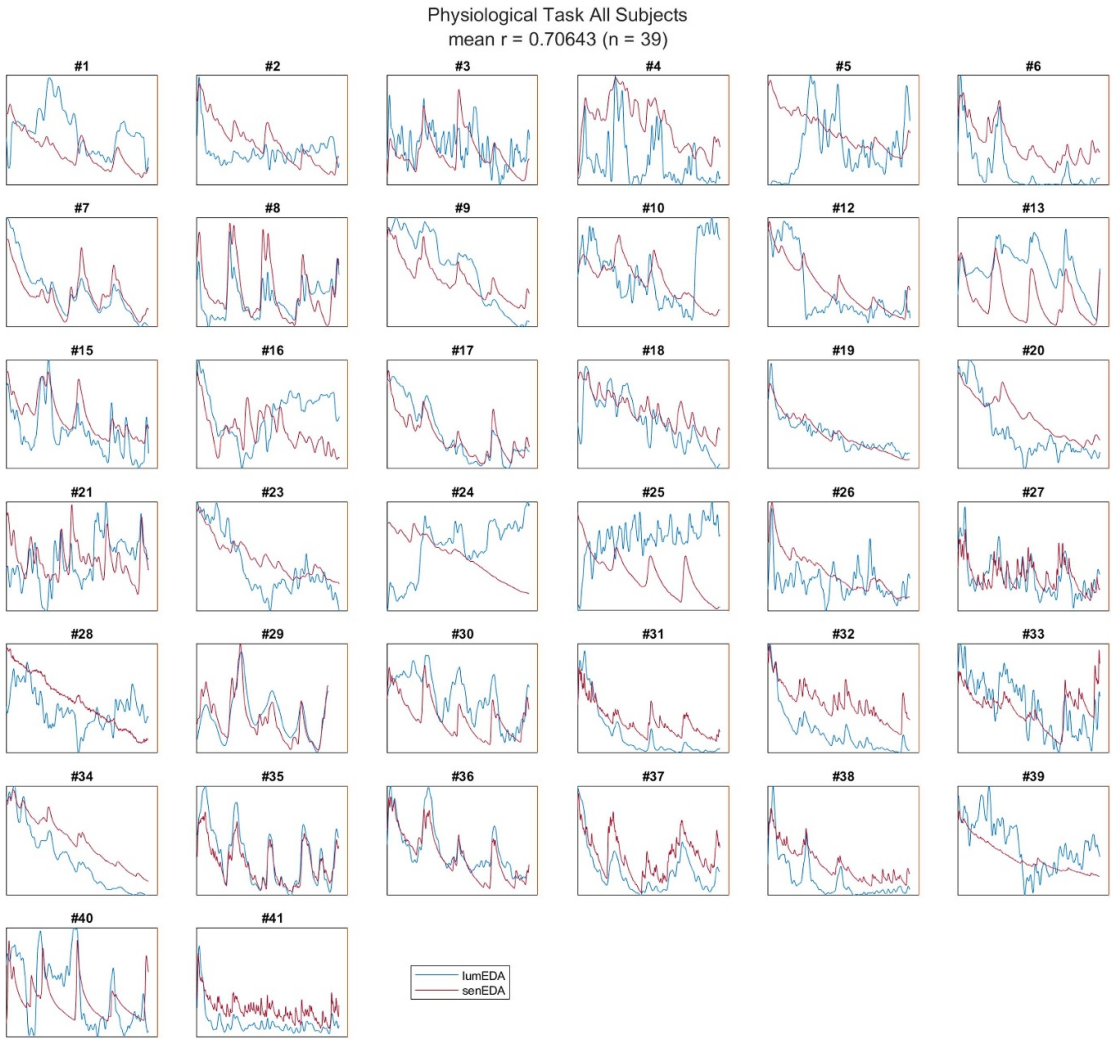

Figure 12. Overview of the SenEDA and LumEDA responses to physiological stimuli (Valsalva Manoeuvre).

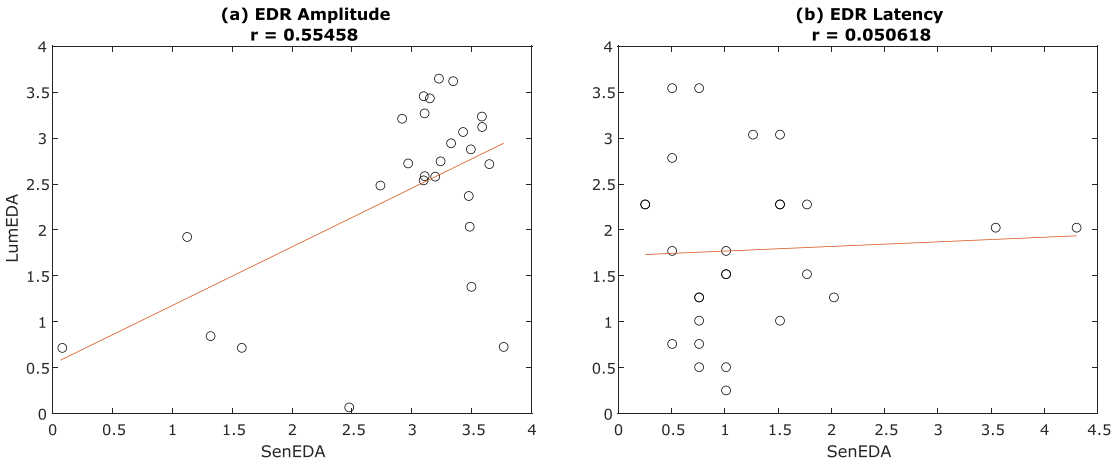

Figure 13. Comparison of (a) EDR amplitudes (b) EDR latencies.

different parts of the measurement, the original camera settings (focus and position) were no longer applicable in later parts of the study. Therefore, only those parts of the measurement that were completed before the hand was moved were included. Some participants also moved their hands slightly between the visual and auditory sections of the measurement explaining the inconsistencies in the LumEDA, since the relative position of the hand with respect to the lights and camera was not the same as it was in the

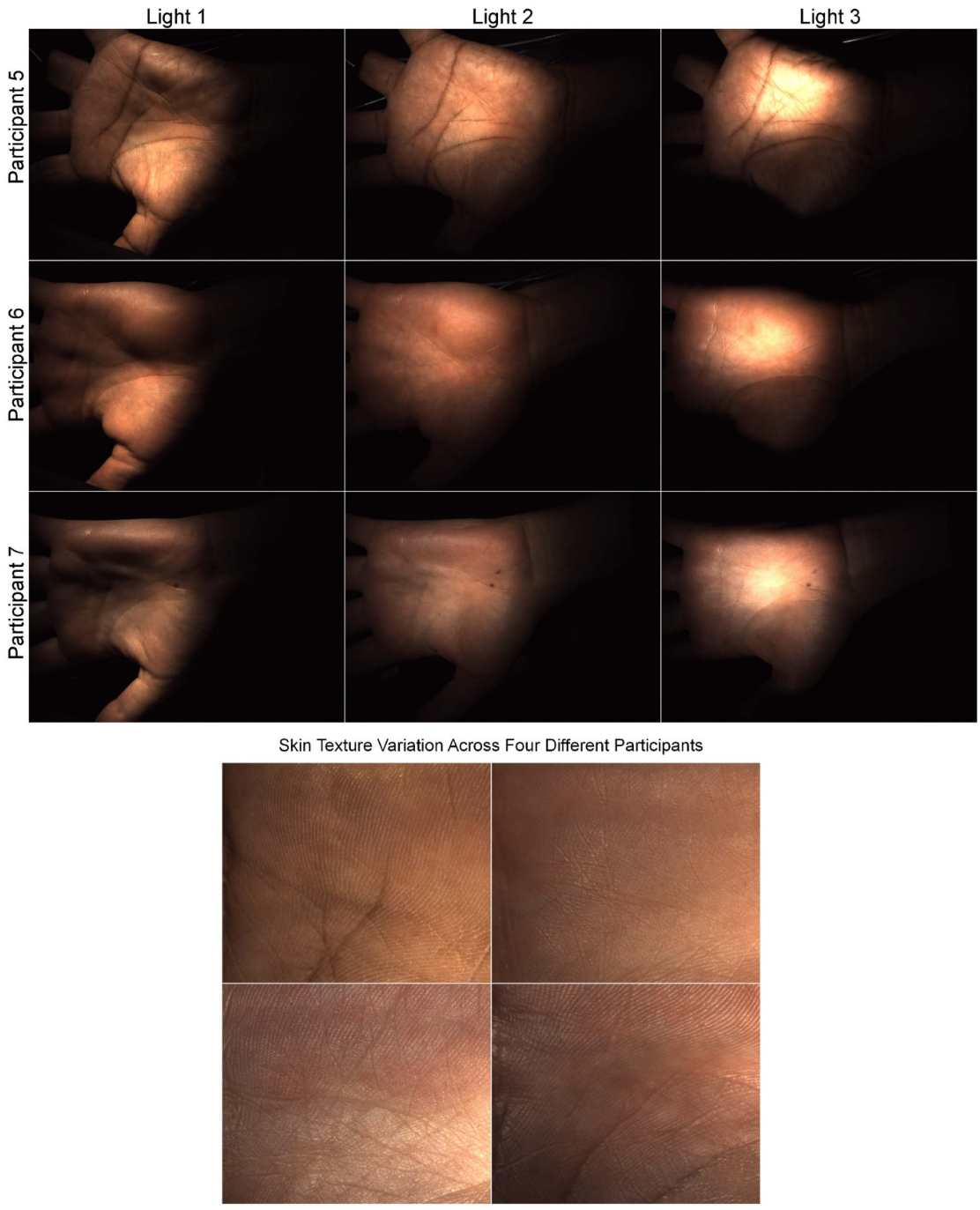

Figure 14. Sample frames from the recordings and the variance in skin type and texture.

beginning. While small amounts of motion do not impact LumEDA significantly, large global motion can potentially completely throw the LumEDA signal off, as seen in the data recorded here as the LumEDA signal is sensitive to the direction of the light.

While a region tracker was used to track a fixed ROI, the nature of the skin texture resulted in the tracker not being very reliable and failing to track a fixed ROI consistently and going off by several pixels and in cases where the tracking fails completely, the ROI had to be reinitialized manually using a visual method, resulting in inconsistencies in the ROI being tracked to synthesize the LumEDA signal.

For a case where the participant kept the hand relatively stable (Participant 21), the contactless signal extracted after performing registration using motion compensation and then fusing frames from all three light sources, did not show a significant difference to the LumEDA signal extracted using a single light source (see figure 16). However, computing optical flow (OF) fields on the fly is computationally expensive especially for high resolutions videos as the one used in the study. Most image fusion algorithms assume that there is little to no motion between the source images but this assumption however, may not hold in real

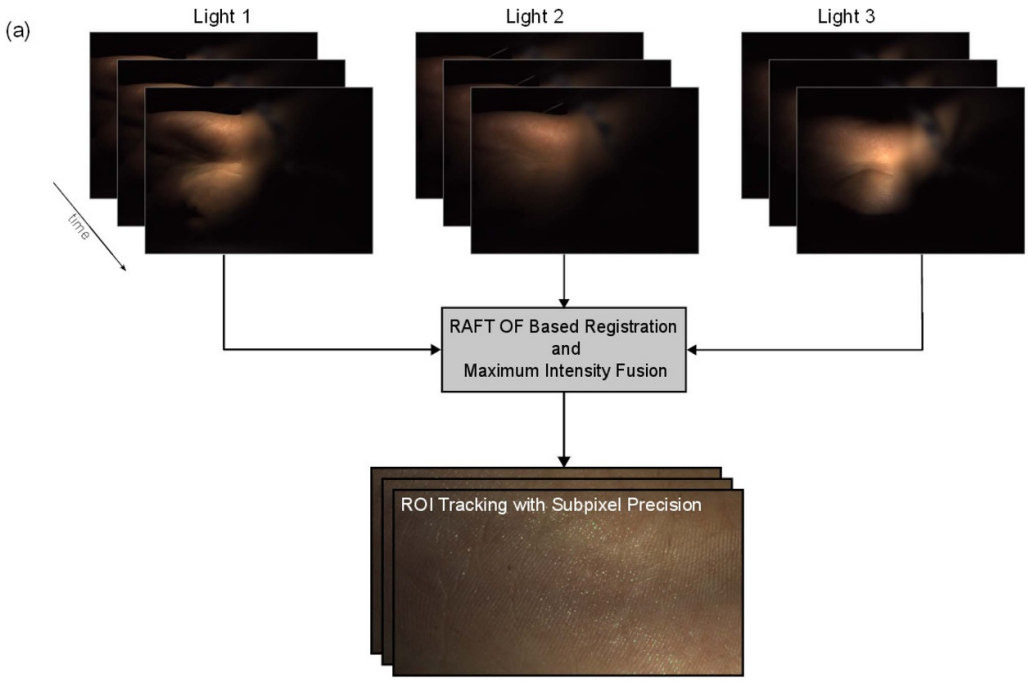

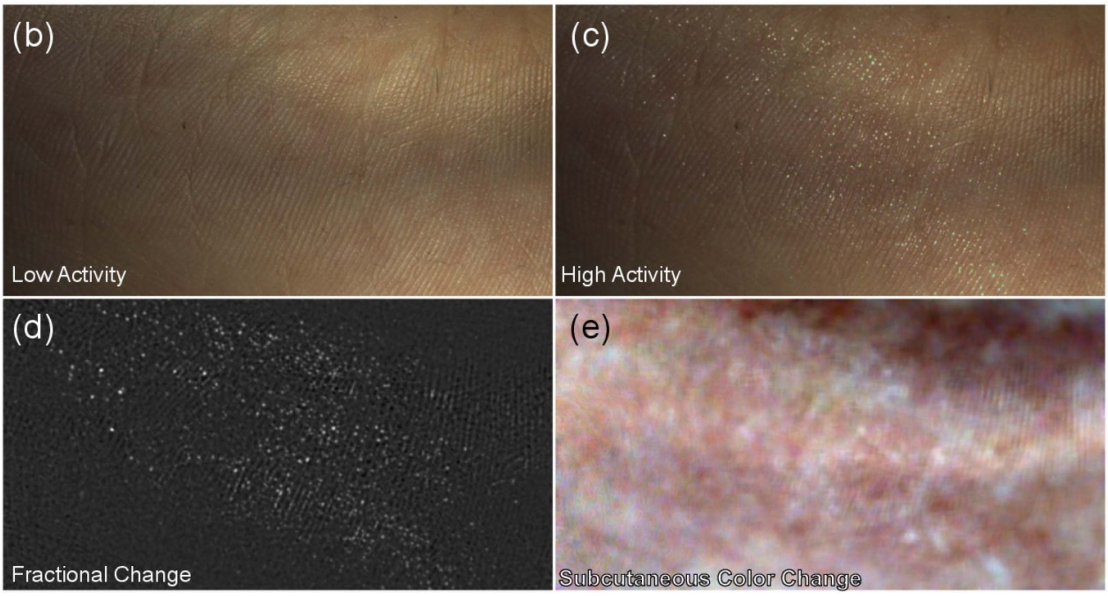

Figure 15. (a) Image registration and fusion. (b) Fused image from low activity period (c) fused image from high activity period (d) fractional change (d) subcutaneous colour change.

world cases, especially when the image resolution is high. Cable based SenEDA is also sensitive to motion. Additionally, motion in general has an impact on EDA. Although the left hand was held stable during the measurement, movement of the right hand could affect the EDA signal measured, due to the symmetric behaviour of EDA (Picard *et al* 2016). These changes, however, would also be apparent in the LumEDA.

4.5. Fractional change using motion compensation and image fusion

Not all participants remained equally still, necessitating some correction for motion. Functional optical imaging in related areas quantifies intensity changes of 2D signals in terms of the fractional change (Δf) (Roome and Kuhn 2019). To this end, an OF based motion compensation method (Flotho *et al* 2022) with RAFT OF back-end (Flotho *et al* 2023) was used. For the sake of computational efficiency, one initial OF field on the downsampled image was computed, motion compensation applied to this, and the process was repeated on the pre-defined ROI. This was done for all three lights, where separate references are kept for each light and separately for each sequence around the events. After frame-wise motion compensation, a

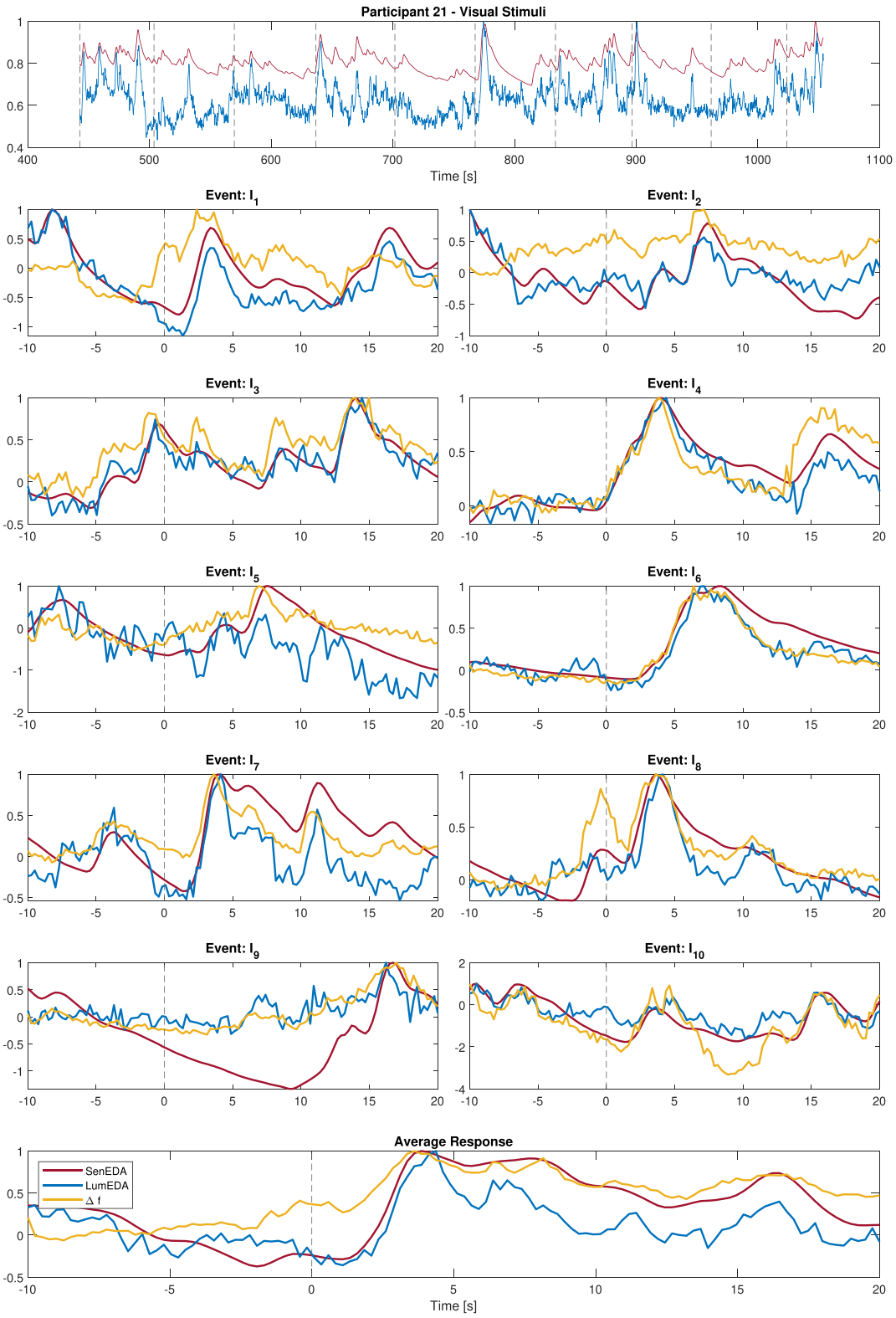

Figure 16. Comparison of SenEDA, LumEDA and fractional change (Δf) (Participant 21 - Visual Stimuli).

fused image consisting of information from all three light sources was synthesized using a maximum intensity heuristic, that is, the brightest pixel among the three is selected. Figure 15 illustrates this procedure along with example frames computed from a low activity period, high activity period and the fractional change.

4.6. Contactless vs contact-based EDA: spatio-temporal aspects

One key aspect to consider in the comparison of SenEDA and LumEDA is the difference in the recording site. While both were recorded from the palm, the location of the recordings was still different, resulting in

potentially different sweat gland behaviour unique to every participant. While sensor-based EDA measurement is well proven and easy to use, the spatial resolution of the sensor-based EDA is poor as compared to image (video) based approaches.

Video based EDA correlates could potentially facilitate the analyses of the spatial distribution of EDA over a larger area, which according to the Multiple Arousal Theory (Picard *et al* 2016) is of great interest in EDA research. The theory states that different brain regions map their activation as different patterns of EDA across the whole body and discusses the importance of creating an EDA map to see where to best measure a specific arousal. Such spatio-temporal electrodermal recordings can also be used to further study conditions such as hyperhidrosis (Wohlrab *et al* 2023).

Another advantage a contactless method provides is the overcoming of issues that occur due to polarization of the electrodes (Boucsein 2012). While the LumEDA signal derived in the scope of this work shows that correlates of EDA can be extracted from using just the greyscale information from the video, better and more robust metrics, that take into account colour variations can be used to estimate EDA correlates.

5. Conclusion

While a proof of concept was already presented for using special illumination techniques for capturing sweat gland activity on the surface of the skin (Bhamborae *et al* 2020), the setup used there was not conducive to long duration measurements. With improvements to the setup and a paradigm that incorporated visual and auditory stimuli, the present study showed that simple image processing approaches can be used to capture sweat gland activity and to estimate psychophysiological and neurocognitive-affective states. The study demonstrated that video-based methods can work effectively under varying experimental conditions. The setup and algorithms used to extract the sweat gland activity in this study were intentionally simple. More robust and accurate metrics can be derived from the video data by incorporating colour information, which correlates with EDA and therefore psychophysiological arousal.

With current progress in augmented and virtual reality, stimuli that can evoke stronger autonomic responses through enhanced immersion (Strauss *et al* 2024) could be used in future studies to further develop contactless methods. The benefit of having spatially resolved EDA estimates from contactless, camera-based sources can enhance research in multisensory experience design, especially when used in conjunction with haptic stimuli (Obrist *et al* 2015, Gatti *et al* 2018). Methods described in this work and in Braun *et al* (2023) and McDuff *et al* (2020) can be adapted for applications such as passenger monitoring (Schneider *et al* 2022).

While contactless correlates are unlikely to replace well-established contact-based measurements in clinical settings, contactless video-based methods provide a non-intrusive alternative for research and non-clinical applications. As camera-based methods provide spatial information, they can complement sensor-based methods for studying sweat gland activity over larger surface areas, enabling spatio-temporal analyses of EDA. This combination will greatly benefit research on the autonomic nervous system and its interaction with the skin.

Data availability statement

The data cannot be made publicly available upon publication because they contain sensitive personal information. The data that support the findings of this study are available upon reasonable request from the authors.

Funding information

This work was partially funded by Federal Ministry of Education and Research through the research grant BMBF-FZ13FH169KX0 : *KINESYMBIOSIS: Integrierte neurotechnologische Architektur zur kontaktlosen Erfassung und Kompensation von Kinetose in selbstfahrenden Fahrzeuge*.

Conflict of interest

The authors declare no conflict of interest.

ORCID iDs

Mayur Bhamborae https://orcid.org/0000-0002-2225-9633
Elena N Schneider https://orcid.org/0000-0002-8902-7693
Philipp Flotho https://orcid.org/0000-0002-8480-0085

Alexander L Francis https://orcid.org/0000-0001-6159-8788
Daniel J Strauss https://orcid.org/0000-0001-8481-499X

References

Baker L B 2019 Physiology of sweat gland function: The roles of sweating and sweat composition in human health *Temperature* **6** 211–59
Baranoski G V and Krishnaswamy A 2010 *Light and Skin Interactions: Simulations for Computer Graphics Applications* (Morgan Kaufmann)
Benjamini Y and Hochberg Y 1995 Controlling the false discovery rate: a practical and powerful approach to multiple testing *J. R. Stat. Soc.* B **57** 289–300
Benjamini Y and Yekutieli D 2001 The control of the false discovery rate in multiple testing under dependency *Ann. Stat.* **29** 1165–88
Benjamini Y and Yekutieli D 2005 False discovery rate–adjusted multiple confidence intervals for selected parameters *J. Am. Stat. Assoc.* **100** 71–81
Bhamborae M J, Flotho P, Mai A, Schneider E N, Francis A L and Strauss D J 2020 Towards contactless estimation of electrodermal activity correlates *2020 42nd Annual Int. Conf. of the IEEE Engineering in Medicine & Biology Society (EMBC)* (IEEE) pp 1799–802
Boucsein W 2012 *Electrodermal Activity* 2nd edn (Springer)
Bradley M M and Lang P J 2007 The international affective digitized sounds (; iads-2): affective ratings of sounds and instruction manual *Technical Report* B-3 University of Florida, Gainesville, Fl
Braun B, McDuff D, Baltrusaitis T and Holz C 2023 Video-based sympathetic arousal assessment via peripheral blood flow estimation *Biomed. Opt. Express* **14** 6607–28
Flotho P, Bhamborae M J, Grün T, Trenado C, Thinnes D, Limbach D and Strauss D J 2021 Multimodal data acquisition at sars-cov-2 drive through screening centers: Setup description and experiences in saarland, germany *J. Biophoton.* **14** e202000512
Flotho P, Heiss C, Steidl G and Strauss D J 2023 Lagrangian motion magnification with double sparse optical flow decomposition *Front. Appl. Math. Stat.* **9** 1164491
Flotho P, Nomura S, Kuhn B and Strauss D J 2022 Software for non-parametric image registration of 2-photon imaging data *J. Biophoton.* **15** e202100330
Freedman L W, Scerbo A S, Dawson M E, Raine A, McCLURE W O and Venables P H 1994 The relationship of sweat gland count to electrodermal activity *Psychophysiology* **31** 196–200
Gatti E, Calzolari E, Maggioni E and Obrist M 2018 Emotional ratings and skin conductance response to visual, auditory and haptic stimuli *Sci. Data* **5** 1–12
Henriques J F, Caseiro R, Martins P and Batista J 2014 High-speed tracking with kernelized correlation filters *IEEE Trans. Pattern Anal. Mach. Intell.* **37** 583–96
Kajiya E, Campos P H O V d, Rizzutto M, Appoloni C and Lopes F 2014 Evaluation of the veracity of one work by the artist di cavalcanti through non-destructive techniques: Xrf, imaging and brush stroke analysis *Radiat. Phys. Chem.* **95** 373–7
Köhler T and Schuschel I 1994 Changes in the number of active sweat glands (palmar sweat index, psi) during a distressing film *Biol. Psychol.* **37** 133–45
Krzywicki A T, Berntson G G and O'Kane B L 2014 A non-contact technique for measuring eccrine sweat gland activity using passive thermal imaging *Int. J. Psychophysiol.* **94** 25–34
Lang P J *et al* 2005 *International Affective Picture System (Iaps): Affective Ratings of Pictures and Instruction Manual* (NIMH, Center for the Study of Emotion & Attention)
McDuff D 2023 Camera measurement of physiological vital signs *ACM Comput. Surv.* **55** 1–40
McDuff D, Nishidate I, Nakano K, Haneishi H, Aoki Y, Tanabe C, Niizeki K and Aizu Y 2020 Non-contact imaging of peripheral hemodynamics during cognitive and psychological stressors *Sci. Rep.* **10** 10884
Nishiyama T, Sugenoya J, Matsumoto T, Iwase S and Mano T 2001 Irregular activation of individual sweat glands in human sole observed by a videomicroscopy *Auton. Neurosci.* **88** 117–26
Nohara K, Ueda Y, Fuji T, Ohmi M and Haruna M 2005 Study of dynamics of sweat glands of human finger tip using all-optical-fiber high-speed oct *2005 Pacific Rim Conf. on Lasers & Electro-Optics* (IEEE) pp 92–93
Obrist M, Subramanian S, Gatti E, Long B and Carter T 2015 Emotions mediated through mid-air haptics *Proc. 33rd Annual ACM Conf. on Human Factors in Computing Systems* pp 2053–62
Picard R W, Fedor S and Ayzenberg Y 2016 Multiple arousal theory and daily-life electrodermal activity asymmetry *Emotion Rev.* **8** 62–75
Posada-Quintero H F *et al* 2016 Highly sensitive index of sympathetic activity based on time-frequency spectral analysis of electrodermal activity *Am. J. Physiol.* **311** R582–91
Posada-Quintero H F *et al* 2016 Power spectral density analysis of electrodermal activity for sympathetic function assessment *Ann. Biomed. Eng.* **44** 3124–35
Posada-Quintero H F and Chon K H 2020 Innovations in electrodermal activity data collection and signal processing: a systematic review *Sensors* **20** 479
Roome C J and Kuhn B 2019 Voltage imaging with annine dyes and two-photon microscopy *Multiphoton Microscopy* pp 297–334
Schneider E N, Buchheit B, Flotho P, Bhamborae M J, Corona-Strauss F I, Dauth F, Alayan M and Strauss D J 2022 Electrodermal responses to driving maneuvers in a motion sickness inducing real-world driving scenario *IEEE Trans. Human-Mach. Syst.* **52** 994–1003
Strauss D J, Francis A L, Vibell J and Corona-Strauss F I 2024 The role of attention in immersion: the two–competitor model *Brain Res. Bull.* **210** 110923
Sutarman S and Thompson M 1952 A new technique for enumerating active sweat glands in man *J. Physiol.* **117** 51–52
Turpin G and Clements K 1993 Electrodermal activity and psychopathology: the development of the palmar sweat index (psi) as an applied measure for use in clinical settings *Progress in Electrodermal Research* (Springer) pp 49–59
Wohlrab J, Bechara F G, Schick C and Naumann M 2023 Hyperhidrosis: a central nervous dysfunction of sweat secretion *Dermatol. Therapy* **13** 453–63
Wu T, Blazek V and Schmitt H J 2000 Photoplethysmography imaging: a new noninvasive and noncontact method for mapping of the dermal perfusion changes *Optical Techniques and Instrumentation for the Measurement of Blood Composition, Structure and Dynamics* vol 4163 (SPIE) pp 62–70
Xiao B, Kogo G, Rutherford G N and Bahoura M 2019 Plasmonic pixel biosensor based on grazing angle illumination and computational imaging *IEEE Sens. J.* **19** 7313–8